

# Production of ZnO thin films used in solar cell with a sol-gel homemade dip coater technique and investigated of their structural, morphological and optical properties

Z. Gültekin\*, C. Akay, N.A. Gültekin, M. Alper

Bursa Uludag University, Bursa, Turkey

E-mail: zafergultekin@uludag.edu.tr

DOI: [10.32523/ejpfm.2023070401](https://doi.org/10.32523/ejpfm.2023070401)

Received: 19.11.2023 - after revision

We designed a homemade dip coater controlled by an Arduino microcontroller to produce semiconductor metal oxide films such as ZnO, CoO, and NiO. The developed device was successfully used to deposit ZnO film on a glass substrate. The structural, surface, and optical properties of the film were investigated. XRD patterns showed that the film is predominantly a hexagonal wurtzite crystalline structure. Scanning electron microscopy (SEM) images showed that the ZnO film was uniformly and homogeneously coated on the glass substrate. EDX analysis confirmed the presence of Zn and O in the film structure. Optical characterization by UV-visible spectrometry showed that the ZnO film has a high transmittance of over 85% in the visible region and absorbs wavelengths in the range of 300–400 nm. Moreover, the band gap of the ZnO film calculated by the Tauc equation was determined as 3.398 eV.

**Keywords:** dip coating; metal-oxide semiconductors; sol-gel; ZnO; band gap

## Introduction

Zinc oxide (ZnO) is an important metal-oxide of the II-VI group that can be used in many devices such as varistors, biosensors, piezoelectric devices, gas sensors, solar cells, organic light-emitting diodes (OLED) etc [1–3]. ZnO is an n-type semiconductor having a direct band gap of 3.37 and a large exciton binding

energy of 60 meV, high transparency, high electron mobility, and high stability and biocompatibility at room temperature [4–6]. On the other hand, since ZnO is transparent in the visible region (400–700), it is frequently used especially in optoelectronic applications.

Today several methods such as chemical vapour deposition, electron beam evaporation, sputtering, molecular beam epitaxy, pulsed laser deposition, spray pyrolysis and sol-gel spin coating [7–10] are used to deposit on any substrate undoped and doped ZnO. Among these coating methods, dip-coating has been always more attractive because of its simplicity, low cost, and facile control [11]. However, in order to make the best high-quality films when coating a substrate, many parameters such as dipping, holding, shrinkage and drying speed must be optimized.

In this study, ZnO thin films were deposited on glass substrate using an homemade dip coater controlled by an Arduino Mega. It was observed that our device could successfully be used to synthesize semiconductor metal oxides such as ZnO, NiO and CoO. Furthermore, it was also found that the structural and optical properties of the films have qualities comparable to those of the materials reported in the literature [12].

## Materials and Methods

### Design and construction of dip coater

First, a dip coater was designed and then constructed by preparing the required equipments. Figure 1 (a) shows the developed dip coater and in figure (b) the 3D design of the dip coater. The substrate to be coated is attached to the movable arm of the dip coater. The substrate must never vibrate during the immersion process. The substrate mounted to an arm, which moves at a constant speed, is immersed into the solution containing the materials to be deposited and kept in it until the desired time. After depositing, the sample is withdrawn at the same and sometimes different speed.

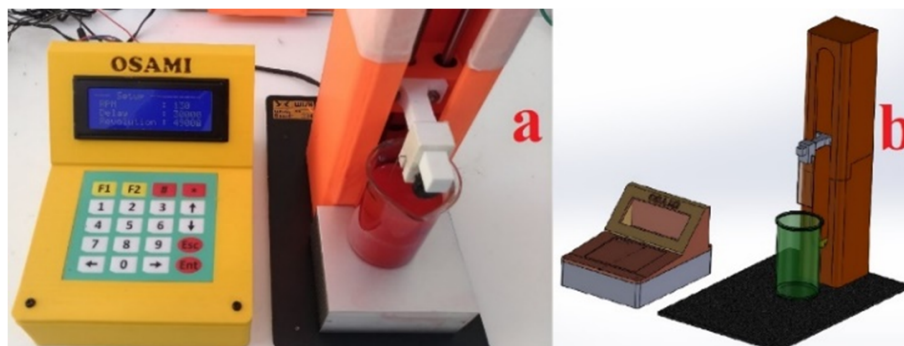


Figure 1. (a) Dip coater with Arduino microcontroller, (b) 3D design of dip coater.

Figure 2 is a schematic diagram of the dip coater. Coating parameters (withdrawn speed, plunge time, and plunge length) entered into the system with the keypad are displayed on the LCD screen. When these parameters are confirmed, Arduino Mega controls the stepper motor with the stepper motor driver. The

substrate to be coated can be dipped one or more times into the solution and removed.

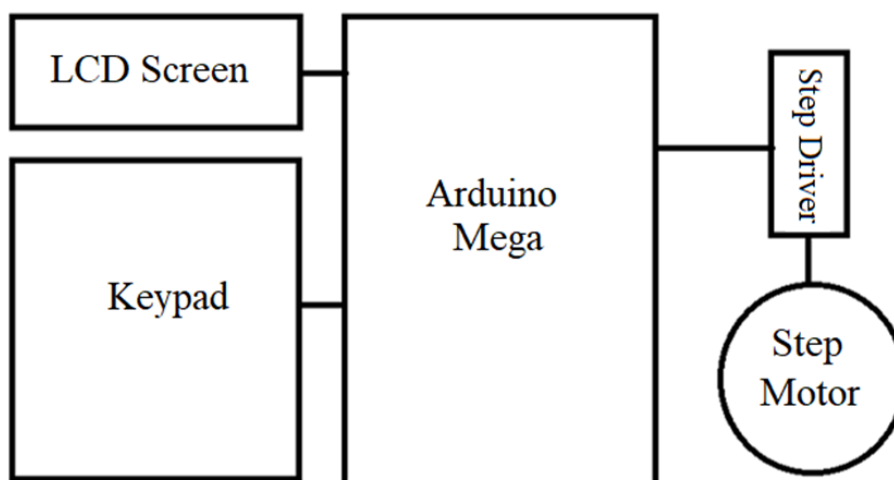


Figure 2. Schematic diagram of the dip coater.

Since there is no limit for the maximum value of the dipping speed of the coater, it is limited to a speed value of 160 mm/s. In this type of coater, the important thing is the stability of the speed rather than the speed during the dipping process. For this reason, a stepper motor is used. Since one step of the shaft used corresponds to 200 turns, there is a height difference of 5  $\mu\text{m}$  per step which is a very good resolution value. If the same operations will be repeated many times, the first operation settings can be saved in memory and called to re-use later. In this way, it can store dozens of working records in its memory. With a USB cable connection, the dip-coater can connect to a computer and can also transfer real-time data.

## ZnO synthesis and coating on a glass substrate

In order to synthesize ZnO films, zinc acetate dihydrate ( $\text{Zn}(\text{CH}_3\text{CO}_2)_2 \cdot 2\text{H}_2\text{O}$ ) (Sigma Aldrich), 2-methoxyethanol (Sigma Aldrich) was employed as the solvent, and monoethanolamine (MEA, Merck) served as a stabilizer.

Initially, 4.40 g of zinc acetate dihydrate was dissolved in 40 ml of methoxyethanol at 60 °C with stirring at 800 rpm for 10 minutes. Subsequently, 1.22 g of MEA was added drop by drop to this mixture, and the resulting blend was stirred for 2 hours at 60 °C. This procedure was also previously applied in [13]. ZnO solution prepared by sol-gel technique was successfully coated on a glass substrate by dip coater technique.

Afterwards, the structural properties of the ZnO coated films were investigated by Bruker AXS/Discovery D8 X-ray diffractometer, surface properties and elemental composition by scanning electron microscopy – energy dispersive x-ray (SEM-EDX) (Carl Zeiss/Gemini 300) and optical properties by UV-VIS spectrophotometer (Flame, Ocean Optics).

## Results and discussion

### Structrual characterisations

Figure 3 shows the XRD patterns of the glass substrate and the ZnO thin film coated on this substrate. The sharp and narrow peaks in the XRD patterns of the ZnO film confirm that the film is highly crystalline. These XRD patterns show that the produced film is polycrystalline with a hexagonal structure (Phase zincite JCPDS 36-1451). XRD pattern of the film has qualities comparable to those of the results reported in [14, 15]. The peaks at positions of about 32.5, 33.5, 36.4, 47.8, 56.4 and 61.8 degrees are indexed as (100), (002), (101), (102), (110) and (103) respectively. The dominant peaks from planes (100), (002) and (101) indicate that ZnO crystallizes in a hexagonal wurtzite structure. The average crystallite size ( $D$ ) of the ZnO film was found using the Debye-Scherrer formula [16] (1):

$$D = (K\lambda) / \beta \cos\theta, \quad (1)$$

where  $K$  is the shape factor (0.9),  $\lambda$  is the wavelength of the  $\text{Cu-K}\alpha$ ,  $\beta$  is the full width at half maximum (FWHM) of the most intense peak of the XRD spectrum, and  $\theta$  is the Bragg angle.

The crystallite size was calculated to be about 59 nm. In addition, the lattice parameters of this structure,  $a$  and  $c$ , were calculated as 0.323 nm and 0.511 nm, respectively.

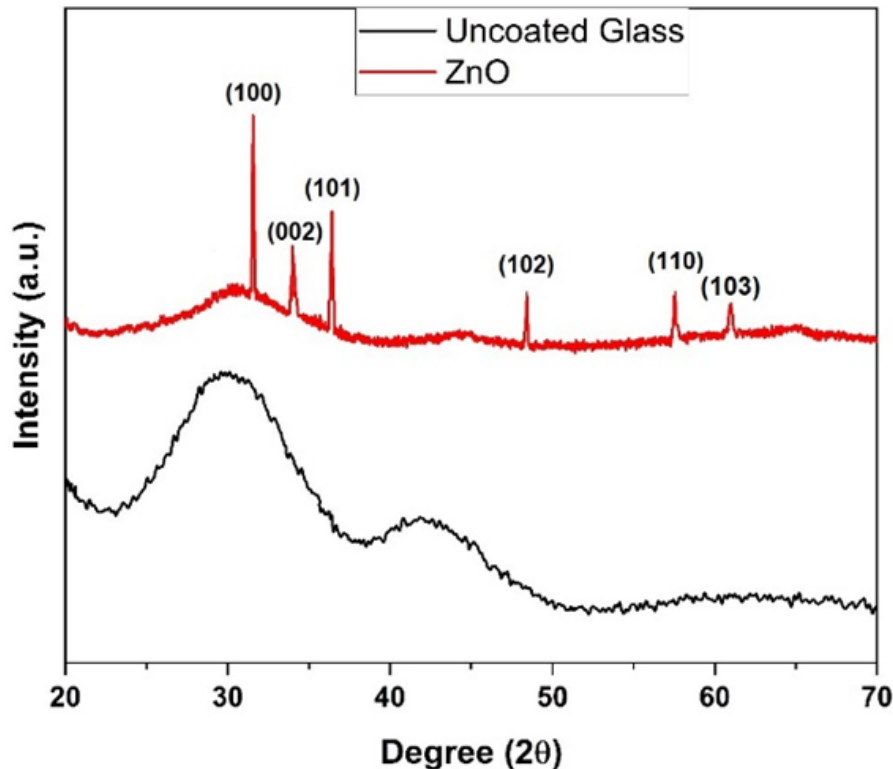


Figure 3. XRD patterns of ZnO thin film and uncoated glass.

Figure 4 shows the surface morphological image of ZnO thin film obtained from a scanning electron microscope (SEM). As seen from the figure, the film

surface have quite uniform, flat and decorat homogeneously coated islands of zinc oxide.

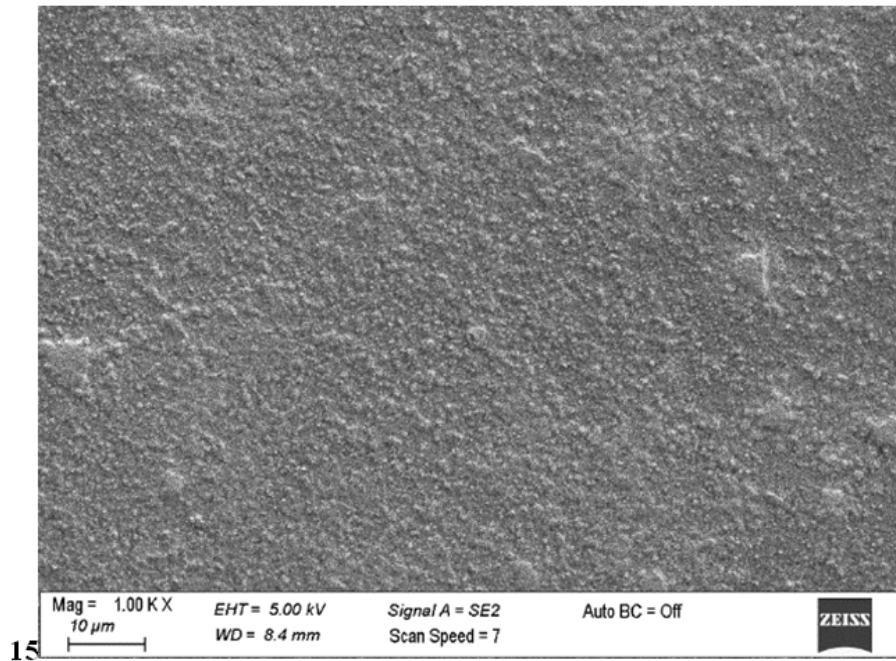


Figure 4. SEM images of ZnO thin film.

Figure 5 shows the EDX data obtained for three different regions of the film surface. The average film composition was found to be 59.20 wt% Zn and 40.80 wt% O. This ratio supports the presence of ZnO in the film.

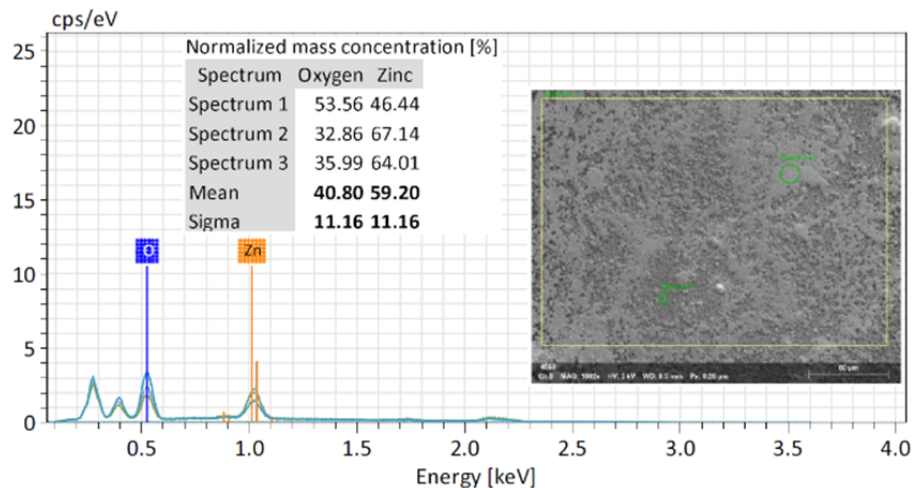


Figure 5. EDX spectra of ZnO thin film.

## Optical characterisations

The optical properties of the films were analyzed with absorbance and transmittance spectra taken in the 300–800 nm range. Figure 6 shows the transmittance change with the wavelength at room temperature. As can be seen from the figure, there is an increasing transmittance edge in the 300–400 nm wavelength range,

reaching around 80–90% transmittance in the wavelength region larger than 400 nm. This high transmittance is crucial for the effective applications such as solar cells where highly transparent and conductive is a major requirement of the electrodes. It is known that the optical transmittance is significantly affected by the scattering on the surface and at the grain boundaries because the scattering at the grain boundaries plays a great role in the change of the optical transmittance [17]. It has been reported in reference [18] that the very steep absorption edge observed around 370 nm is associated with high crystal quality, which can increase the luminescence efficiency.

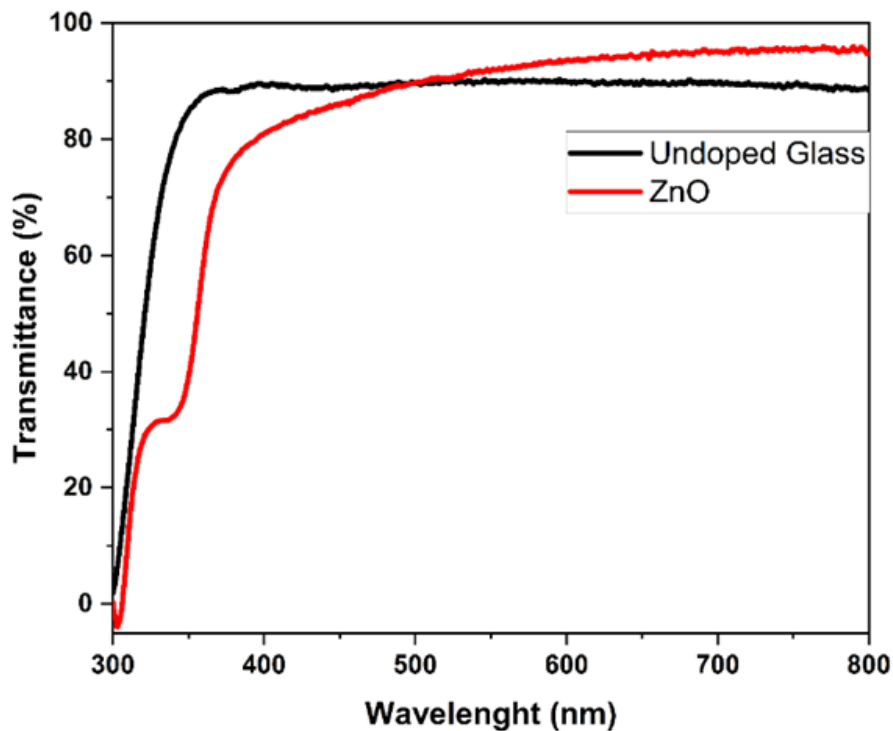


Figure 6. Transmittance spectra of ZnO thin film and uncoated glass.

The absorbance spectra of ZnO thin film at room temperature are shown in Figure 7. The ZnO film absorbs light in the wavelength range of 300–400 nm (UV region) and almost does not absorb light with wavelengths greater than 400 nm. In addition, the sharp absorbance peaks in the UV region indicate that photoelectrons are excited from the valence band (VB) to the conduction band (CB) at these wavelengths [19].

Figure 8 shows a plot of  $(\alpha h\nu)^2$  versus photon energy  $h\nu$  (eV) for the ZnO film.  $\alpha$  is the absorbance coefficient and was calculated by (2).

$$\alpha = (2.303 \cdot A)/t, \quad (2)$$

where,  $A$  is absorbance and  $t$  is film thickness. The thickness of the ZnO film was measured to be approximately 110 nm.

The optical bandgap ( $E_g$ ) is expressed by the  $T_{auc}$  equation [20] (3) and is found by extrapolating the linear part in Figure 8 to the x-axis (energy axis).

$$\alpha h\nu = B(h\nu - E_g)^{1/2}, \quad (3)$$

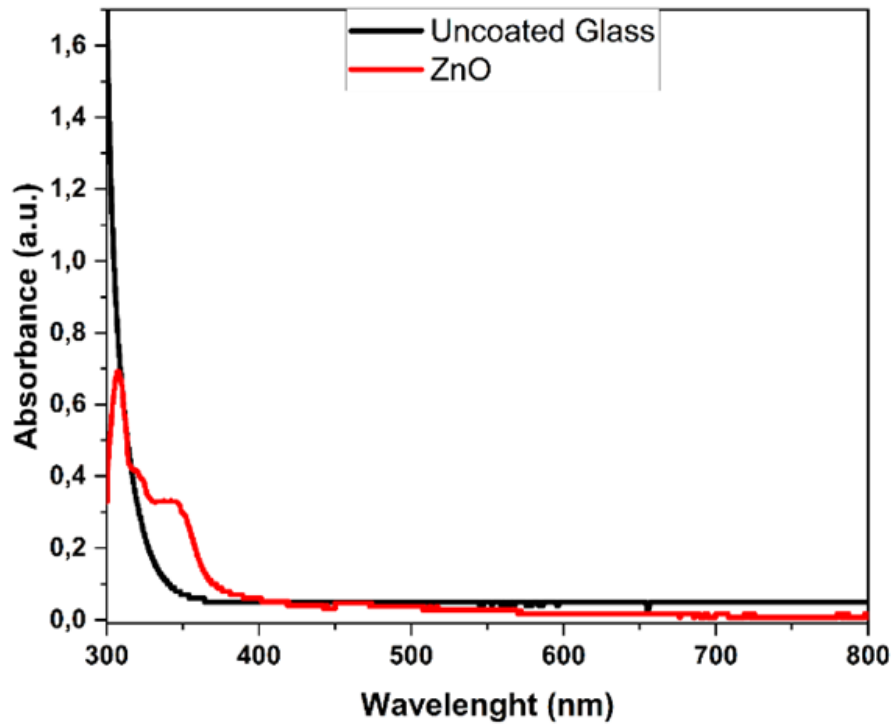


Figure 7. Absorbance spectra of ZnO thin film and uncoated glass.

where  $B$  is a constant of proportionality. According to equation (3), the  $E_g$  for the ZnO film was found to be about 3.398 eV. This value is in agreement with other reported results [21, 13].

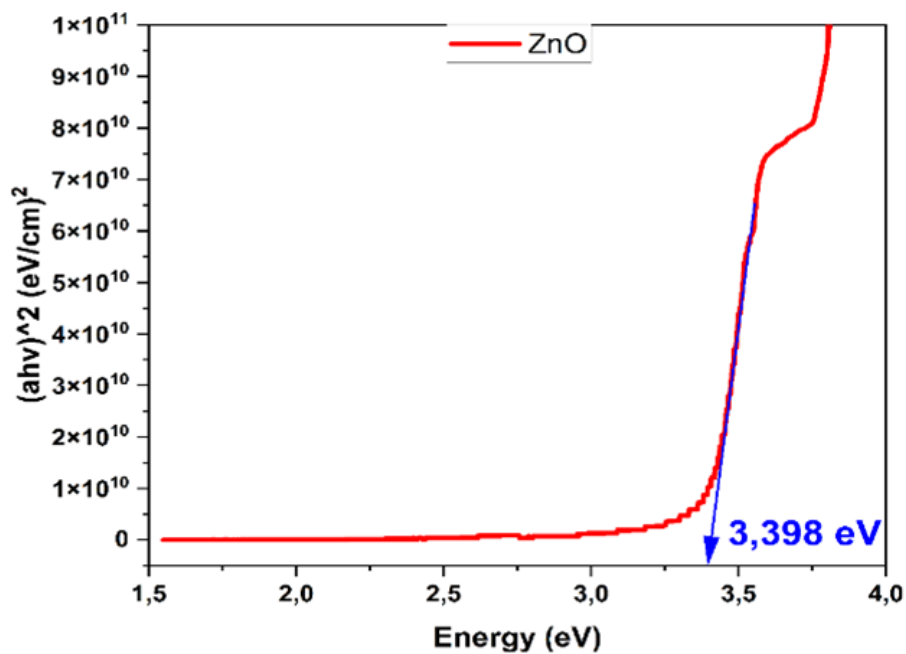


Figure 8. Band gaps of ZnO thin film.

## Conclusion

An homemade dip coater device controlled by an Arduino microcontroller was developed to fabricate metal oxides such as ZnO. Using our device, as an example, ZnO thin film was successfully coated on glass substrates by sol-gel technique. The XRD patterns and EDX analysis support the crystal quality and the formation of ZnO film. The morphological structure by SEM demonstrated that the film has smooth and uniform surfaces. The film has high transmittance values of over 85% in the visible region and exhibits an absorbance spectrum in the 300–400 nm range.

## References

- [1] X. Sun and H. Kwork, *J. Appl. Phys.* **86** (1999) 408. [[CrossRef](#)]
- [2] C.M. Vladut et al., *Journal of Nanomaterials* **2019** (2019) 6269145. [[CrossRef](#)]
- [3] P. Soundarrajan and K. Sethuraman, *RSC Advances* **5** (2015) 44222–44233. [[CrossRef](#)]
- [4] M. Willander et al., *Nanotechnology* **20** (2009) 332001. [[CrossRef](#)]
- [5] A. Raidou et al., *Moroccan Journal of Condensed Matter* **12**(2) (2010) 125–130. [[WebLink](#)]
- [6] H. Kim et al., *Thin Solid Films* **377-378** (2000) 798–802. [[CrossRef](#)]
- [7] M.H.N. Assadi, D.A.H. Hanaor, *Journal of Applied Physics* **113** (2013) 233913. [[CrossRef](#)]
- [8] Hsin-Chiang You, Yu-Hsien Lin, *International Journal of Electrochemical Science* **7** (2012) 9085–9094. [[CrossRef](#)]
- [9] S. Sharma et al., *Electronic Materials Letters* **11** (2015) 1093–1101. [[CrossRef](#)]
- [10] E. Heredia et al., *Applied Surface Science* **317** (2014) 19–25. [[CrossRef](#)]
- [11] D. Grosso, *J. Mater. Chem.* **21** (2011) 17033–17038. [[CrossRef](#)]
- [12] F. Dabir et al., *Journal of Sol-Gel Science and Technology* **96** (2020) 529–538. [[CrossRef](#)]
- [13] Z. Gültekin et al., *Journal of Materials Science: Materials in Electronics* **34** (2023) 438. [[CrossRef](#)]
- [14] R.K. Sharma et al., *Adv. Nat. Sci: Nanosci. Nanotechnol.* **3**(3) (2012) 035005. [[CrossRef](#)]
- [15] S.A. Kamaruddin et al., *Appl. Phys. A* **104** (2011) 263–268. [[CrossRef](#)]
- [16] Q. Humayun et al., *Journal of Nanomaterials* **2013** (2013) 792930. [[CrossRef](#)]
- [17] L. Xu et al., *Journal of Alloys and Compounds* **548** (2013) 7–12. [[CrossRef](#)]
- [18] K. Nadarajah et al., *Journal of Nanomaterials* **2013** (2013) 146382. [[CrossRef](#)]
- [19] M. Bouloudenine et al., *Catalysis Today* **113**(3–4) (2006) 240–244. [[CrossRef](#)]
- [20] P. Gu et al., *Journal of Materials Science: Materials in Electronics* **29** (2018) 14635–14642. [[CrossRef](#)]
- [21] M.R. Islam et al., *Surfaces and Interfaces* **16** (2019) 120–126. [[CrossRef](#)]